85
Research paper
Doi 10.61892/STP202601007B
ISSN 2566-4484

STEPGRAD
СТЕПГРАД

Konstantinos Bellos, Aristotle University of Thessaloniki, costas.bellos@hotmail.com
Ion-Anastasios Karolos, Aristotle University of Thessaloniki, ikarolos@topo.auth.gr
Stylianos Bitharis, Aristotle University of Thessaloniki, smpithar@topo.auth
Athanasios Iliodromitis, University of West Attica, a.iliodromitis@uniwa.gr

EVALUATING ACCURACY AND RELIABILITY OF MODERN 3D RECONSTRUCTION AND MEASUREMENT TECHNIQUES: A CASE STUDY OF A BYZANTINE BATH

Abstract:

Recent advances in 3D reconstruction techniques, including Terrestrial Laser Scanning (TLS), SLAM-based systems, and mobile LiDAR, have improved heritage documentation practices. This study evaluates the geometric accuracy of Leica BLK360, GeoSLAM ZEB-REVO, FJD TRION™ S1, and iPhone 12 Pro using a UNESCO-listed Byzantine Bath monument, with FARO Focus 3D as the reference dataset. Accuracy was assessed through C2C and M3C2 analyses on a 3 × 3 m floor subset and two vertical sections. Floor results showed mean deviations of 4.7–25 mm, with the iPhone 12 Pro yielding the lowest z-axis mean error, while BLK360 produced the most stable dataset. Section analysis indicated mean differences of 8–22 mm, with BLK360 demonstrating the closest agreement to reference data. Overall, all systems achieved centimeter-level accuracy, with mean deviations ranging from 4.7 mm to 25 mm, while the standard deviation of distances reached up to approximately 30 mm depending on the instrument and the analysed geometry.

Keywords: 3D Modelling, LiDAR, SLAM, Terrestrial Laser Scanning, Point Cloud Comparison, Cultural Heritage

ПРОЦЕНА ТАЧНОСТИ И ПОУЗДАНОСТИ САВРЕМЕНИХ ТЕХНИКА 3Д РЕКОНСТРУКЦИЈЕ И МЕРЕЊА: СТУДИЈА СЛУЧАЈА ВИЗАНТИЈСКОГ КУПАТИЛА

Сажетак:

Недавни напредак у техникама 3Д реконструкције, укључујући терестријално ласерско скенирање (TLS), системе засноване на SLAM-у и мобилни LiDAR, унапредио је праксе документовања културног наслеђа. Ова студија процењује геометријску тачност уређаја Leica BLK360, GeoSLAM ZEB-REVO, FJD TRION™ S1 и iPhone 12 Pro на примеру византијског купатила са UNESCO листе, при чему је FARO Focus 3D коришћен као референтни скуп података. Тачност је процењена применом C2C и M3C2 анализа на подскупу пода димензија 3 × 3 m и на два вертикална пресека. Резултати за под показали су средња одступања од 4,7 до 25 mm, при чему је iPhone 12 Pro остварио најмању средњу грешку по z-оси, док је BLK360 произвео најстабилнији скуп података. Анализа пресека указала је на средње разлике од 8 до 22 mm, при чему је BLK360 показао највеће слагање са референтним подацима. Укупно посматрано, сви системи су постигли тачност на нивоу центиметра, при чему су средња одступања износила од 4,7 mm до 25 mm, док је стандардна девијација достизала приближно 30 mm, у зависности од инструмента и анализиране геометрије.

Кључне речи: 3Д моделовање, LiDAR, SLAM, терестричко ласерско скенирање, поређење облака тачака, културно наслеђе

1. INTRODUCTION

The history of Thessaloniki dates to the Hellenistic era and has persisted without interruption up to the present day. Its evolution is mainly associated with the city's Byzantine heritage, and the walled city along with its monuments could be characterised as an open-air Byzantine Museum. All of the city's landmarks, including the Byzantine, Post-Byzantine, and Ottoman monuments, have been officially designated as historical landmarks. Additionally, fifteen (15) of the early Christian-Byzantine monuments were added to the UNESCO World Heritage List in 1988 (UNESCO code 456). One of the most iconic of them is the Byzantine Bath of Thessaloniki, which is the study object of the current paper.

The Byzantine Bath is located on the edge of Thessaloniki's Upper Town, in the Koule Kafe district, within the historic fortified core of the city, 62 m above the sea level. It is very close to the Byzantine cistern in Olympiados St. and the church of the Archangels, and it's the only public Byzantine bath currently preserved in Thessaloniki (Latitude 40° 28′ 23″ N, longitude 22° 57′ 10″ E). (Figure 1). The surrounding area consists of residential buildings.

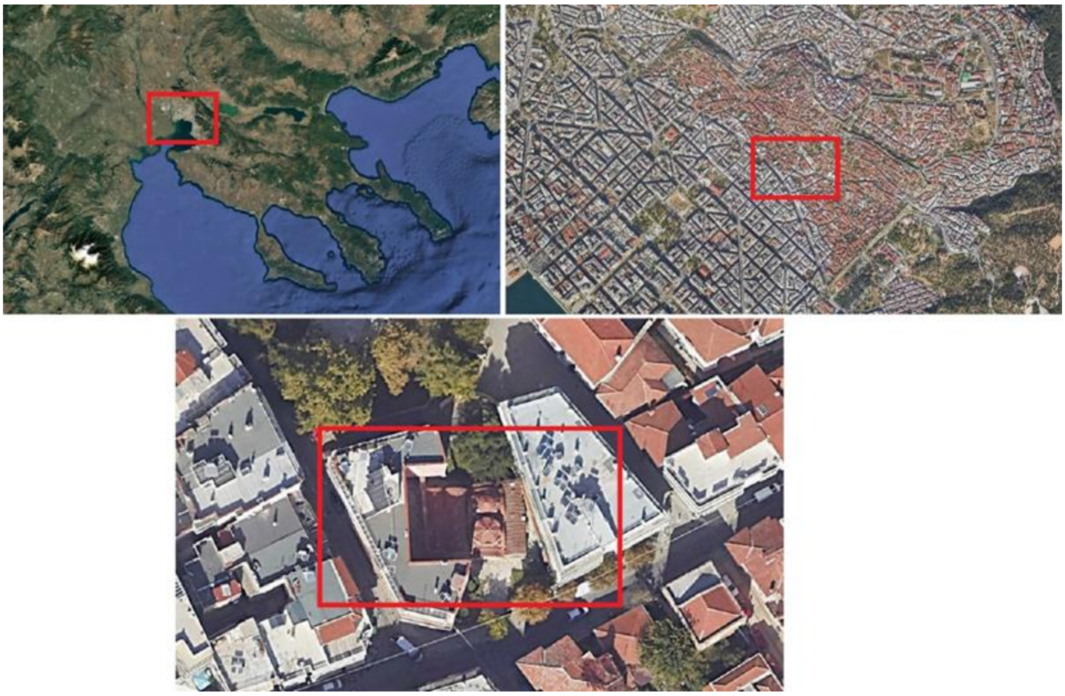

Figure 1. Location of the Byzantine Bath (Diagrams created by the author based on Google Earth imagery).

This building, has a rectangular configuration of 17m x 12.50m, is distinguished by the inclusion of an antechamber, warm-room (tepidarium), hot-room (caldarium), and water reservoir, which are essential features of a typical Roman bathhouse, as illustrated in Figure 2.

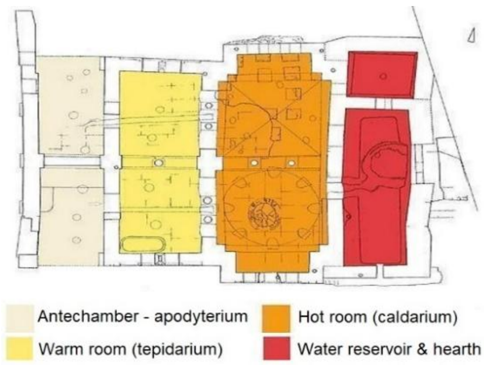

Figure 2. Plan of Byzantine Bath (Drawing by architects Fani Revithiadou and Konstantinos T. Raptis [1]).

It is thought to date back to the 13th century, while it continued to operate during the Ottoman period, during which it underwent several modifications and became known as Kule Hammam, a name derived from the district in which it is built. Its use as baths was discontinued during the 1940s. In 1952, it was designated as a protected monument, and during the 1970s the first restoration works were carried out in the bath area. As a consequence of the 1978 earthquake, structural support and stabilization works were subsequently undertaken. In 2002, the building was highlighted and promoted through initiatives of the 9th Ephorate of Byzantine Antiquities. Following a new phase of restoration works that began in the early 2010s, the monument was reopened to the public in 2015.

It is characterized by its confined interior spaces, a complex vault geometry and irregular masonry surfaces. These characteristics make the monument, an appropriate and challenging case study for evaluating the accuracy and reliability of different 3D reconstruction technologies under realistic heritage documentation conditions. This research aims to provide clear insights into the 3D measurement capabilities of modern instruments, devices, and methods for cultural heritage preservation purposes.

2. METHODS & MATERIALS

This section provides a comprehensive delineation of the techniques, instrumentation, and analytical procedures adopted in the present investigation. The primary objective of this study is to quantitatively evaluate the point cloud outputs generated by Simultaneous Localization and Mapping (SLAM) algorithms against those acquired via Terrestrial Laser Scanners (TLS). The analysis focuses on two TLS systems and three distinct SLAM-based solutions. The comparative assessment encompasses a spectrum of instrumentation, extending from high-precision industrial surveying devices to more accessible LiDAR platforms, including those integrated in consumer-grade mobile devices such as the iPhone 12 Pro Max [2], [3]. To facilitate a rigorous comparative evaluation between TLS and SLAM point clouds, the study implements a structured methodological framework comprising the following key components: (i) Point cloud registration, in which datasets are co-registered within a common reference frame. This process employs Iterative Closest Point (ICP) algorithms as a fine-registration mechanism to reduce residual discrepancies between corresponding geometric surfaces. (ii) Quantitative accuracy assessment, based on cloud-to-cloud distance metrics and associated statistical analysis. This includes computation of global and local deviation measures (e.g., mean error, standard deviation, root mean square error) to characterize agreement between SLAM and TLS point clouds. (iii) Evaluation of systematic biases, trajectory drift, and localization errors inherent in SLAM outputs. Particular emphasis is placed on examining the effects of loop closure, and cumulative drift over extended acquisition paths, which are known to influence SLAM performance in large-scale or feature-sparse environments.

2.1. PRINCIPLES OF LASER SCANNING & SLAM SYSTEMS

Laser scanning devices, such as Terrestrial Laser Scanners (TLS), function by firing laser beams towards a surface and measuring the time it takes for the laser pulses to return. This procedure facilitates the generation of intricate 3D point clouds, accurately capturing the geometry and terrain of the scanned surroundings [4], [5]. The reference coordinate system of the laser scanner corresponds to the electro-optical center of the measuring head of the instrument. The primary measurements of the laser scanner are conducted in a spherical coordinate system, as is the case in conventional topographic surveys. The scanner operates within a spherical coordinate system, utilizing regular increments in horizontal (Δ_θ) and vertical (Δ_υ) angles. The TLS captures reflections from surfaces, recording the horizontal angle (θ) and vertical angle while calculating the range (ρ) to the object surface, considering the TLS as the coordinate system's center.

The point cloud is defined at consistent intervals of θ and υ in spherical coordinates. In contemporary systems, the point cloud with n acquisitions is typically expressed in Cartesian coordinates, computed from the measured spherical coordinates using Eq.1:

$$[x_i\ y_i\ z_i\ ]_{i=1\cdots n} = [\rho_i cos\, \upsilon_i cos\, \theta_i\ \rho_i cos\, \upsilon_i sin\, \theta_i\ \rho_i sin\, \upsilon_i\ ]_{i=1\cdots n} \tag{1}$$

The Cartesian representation of the 3D point cloud is disorganized. Conversely, the spherical coordinates of the point cloud are derived from Cartesian coordinates, as explained in Eq.2:

$$[\theta_i \; v_i \; \rho_i \;]_{i=1\cdots n} = \left[tan^{-1}\left(\frac{y_i}{x_i}\right) \; tan^{-1}\left(\frac{z_i}{\sqrt{x_i^2+y_i^2}}\right) \; \sqrt{x_i^2 + y_i^2 + z_i^2} \right]_{i=1\cdots n} \quad (2)$$

SLAM systems utilise a blend of sensors, including LiDAR and cameras, to simultaneously navigate and create a real-time map of an area. The fundamental idea is the ongoing adjustment of the system's location while concurrently generating a map of the environment. SLAM is especially beneficial in situations where GPS signals may be erratic or inaccessible, offering a precise option for locating and mapping.

2.2. DATA COLLECTION & REFERENCE ESTABLISHMENT

In order to carry out our investigation, we utilised the Faro Focus 3D Laser Scanner to make several scans of the monument from different locations. The reference dataset consisted of these measurements, which enabled us to utilise cloud-to-cloud (C2C) algorithms [6] and evaluate distances using different methodologies [7] between metric data gathered from different systems. We chose the FARO Focus 3D as our reference system due to its outstanding precision in capturing point cloud data. The FARO system's distance range accuracy of 2 mm solidifies its reputation as a dependable tool for precision measurements. The major characteristics of the instruments used in our investigation are presented in Table 1. These specifications were obtained directly from the manufacturers [8], [9], [10]. The purpose of providing this comprehensive information is to ensure that readers have a precise comprehension of the equipment's functionalities, hence promoting transparency in our study methodology.

2.3. TERRESTRIAL LASER SCANNERS

Terrestrial Laser Scanners (TLS) are particularly useful for monument documentation in surveying or forest applications [11], [12], [13]. Monuments are structures that have cultural, historical, or archaeological significance, and accurate geometric documentation of these objects is critical for preservation and research purposes. TLS technology enables surveyors to capture high-resolution three-dimensional data of monuments with great accuracy and detail, providing a permanent record of their current condition. The resulting point cloud data can be used to create detailed 3D models, which can be used for analysis, restoration, and replication purposes. TLS is also helpful in creating detailed documentation of the surrounding environment, which can help provide context for the monument and aid in its interpretation. Overall, the use of TLS in monument documentation enables surveyors to produce accurate and detailed records of monuments.

2.4. SIMULTANEOUS LOCALIZATION & MAPPING - SLAM

In surveying engineering, SLAM systems can be used to create accurate mapping of human structures and the natural environment. SLAM was developed as a technology for autonomous vehicles that enables them to create maps and localize their positions on those maps [14]. Most specifically LiDAR SLAMs can be used to combine data from a laser emitter-receiver with IMU corrections over time. This data can then be used to generate 3D point clouds, which can be further processed to create detailed mapping, floor plans, and elevation models. SLAM systems in surveying are particularly useful in situations where traditional surveying methods are impractical or unsafe, such as in areas with difficult terrain, absence of GNSS signal, or hazardous conditions. SLAM technology is faster and easier to capture data in a fraction of the time required for traditional surveying methods. Also, this kind of technology can operate in quasi real-time, allowing surveyors to quickly collect 3D data of large areas with relatively low cost and high accuracy.

Table 1. Specifications of main equipment characteristics

Distance measurement system	FARO focus 3D	Leica Blk360	iPhone 12 Pro	GeoSLAM ZEB-REVO	FJD TRION ™ S1
Maximum range (m)	120	45	5	30	120
Max. scan rate (pts/sec)	976.000	680.000	-	43.200	320.000
Resolution settings	1/8 or 1/10 - Indoors and small, outdoor spaces	4 (6/12/25/50 mm @ 10 m)	3 modes (low/ medium/high)	30 mm	-
Laser wavelength (nm)	905	830	940	905	905

3. RESULTS

In the post-processing part of the Laser Scanning measurements, we used several software tools [15]. The twenty-one (21) point clouds from the Faro Focus 3D were processed with the Faro Scene software application. The scans were aligned and registered using Iterative Closest Point (ICP) algorithm providing a cloud-to-cloud registration to create a unified 3D model of the monument [16], [17]. The accuracy of the registration is 3.5 mm. For the Leica BLK360 scans the post-processing software that was used is Cyclone Register 360 using also the ICP algorithm. Twenty (20) scans were performed to capture the environment of interest with over 50% overlap and a registration accuracy of 5 mm. The data from the Geoslam Zeb REVO system were processed from the Geoslam hub post-processing environment and the results are a 3D geometric model of the monument with 5.5 million number of points acquired in a short period of time (5-7 minutes). The accuracy (internal) of the automated registration procedure was not produced by the Geoslam hub application, hence the accuracy (external) will be evaluated through the comparison with the ground-truth data. The data from the FJD TRION™ S1 system were processed in the FJDynamics software and provided a dataset of 3.7 million points in almost the same duration. Finally, the post-processing of the data captured from the LiDAR sensor of the iPhone 12 Pro [18] is an automated and user-friendly procedure which is performed almost simultaneously with the data captured in an iOS application (i.e. 3D Scanner app - link: https://apps.apple.com/us/app/3d-scanner-app/id1419913995 [19]).

4. DISCUSSION

This section presents the methodological framework adopted to evaluate the efficacy and accuracy of the different instruments and acquisition techniques used to document specific segments of the monument, as illustrated in Fig. 3. The analysis follows a structured workflow comprising data acquisition, preprocessing and registration, definition of a reference dataset, and quantitative validation through consistent accuracy metrics. All datasets were acquired according to the recommended operational procedures of each system. Following acquisition, the data were processed using a standardized workflow to ensure comparability among systems. This included filtering, noise reduction, alignment, and registration within a common reference framework. Whenever possible, consistent processing parameters were applied in order to minimise methodological bias and ensure that observed differences could be attributed primarily to the performance of the instruments rather than to variations in data handling.

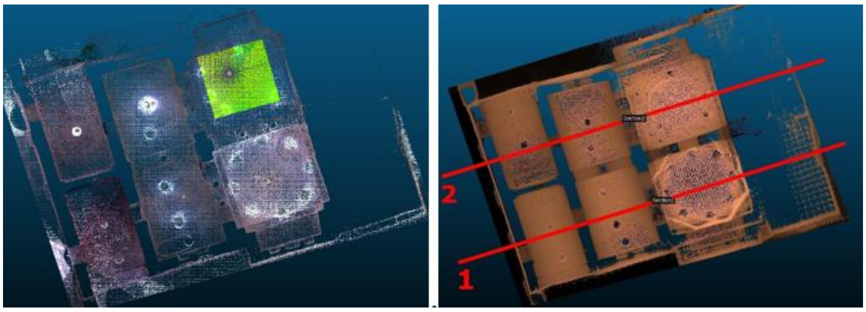

Figure 3. Location of segmented positions (Drawings created in CloudCompare by the author).

The selection of the analysed parts of the monument was undertaken deliberately to represent distinct geometric and operational conditions.

The floor area was chosen because it constitutes a predominantly flat and geometrically simple surface. Planar surfaces are particularly suitable for evaluating systematic deviations, vertical accuracy, and noise levels, as even minor undulations or distortions become readily detectable. This configuration therefore provides a controlled environment for assessing precision and surface regularity.

The section analysis was performed to examine the spatial distribution of points and the capability of each instrument to capture geometric discontinuities and elevated features. By extracting vertical cross-sections, it becomes possible to directly observe differences in point density, completeness, and the representation of higher architectural elements. This approach allows for a clearer understanding of how each system records complex geometries and how measurement quality may vary with height or accessibility.

Finally, the Multiscale Model-to-Model Cloud (M3C2) method was applied to evaluate geometric deviations at both local and global scales. At the façade level, the method enables a detailed assessment of each instrument's ability to record fine architectural features and surface details. At the full-building scale, it allows the identification of cumulative or systematic errors, particularly those associated with SLAM-based systems, where trajectory drift, IMU inaccuracies, and algorithmic error propagation may become significant. The multiscale comparison therefore provides insight into both local detail fidelity and overall geometric consistency.

A reference dataset acquired with a FARO terrestrial laser scanner was used as the validation benchmark. The selection of this dataset was based on the intrinsic characteristics of terrestrial laser scanning technology, which provides high measurement accuracy and a significantly higher point density compared to the other tested systems. The FARO scanner ensures stable acquisition geometry, dense spatial sampling, and reduced susceptibility to cumulative trajectory errors, thereby making it suitable to serve as a benchmark for comparative analysis. Its role in this study is to provide a consistent reference against which deviations from the other systems can be quantified. Nevertheless, it is acknowledged that even this dataset is not entirely free from uncertainty, as potential sources of error may arise from instrumental limitations, registration residuals, and environmental conditions during acquisition. Consequently, the reported deviations should be interpreted as relative differences with respect to the reference dataset rather than as absolute measures of truth.

The accuracy and reliability of each system were evaluated using consistent quantitative criteria applied uniformly across all datasets. These criteria include geometric deviation from the reference dataset, statistical dispersion of distances, point density and distribution, surface roughness and noise characteristics, completeness of data capture, and the presence of systematic distortions. By maintaining methodological consistency in the evaluation process, the analysis provides a transparent and comparable assessment of system performance and supports reasoned recommendations regarding the suitability of each instrument for specific documentation scenarios within the monument. Quality control of the datasets was ensured through several procedures, including multi-scan overlap (>50%), ICP-based registration, evaluation of registration residuals (3.5 mm for FARO and 5 mm for BLK360), and comparison against the FARO Focus 3D reference dataset, which has a manufacturer-specified ranging accuracy of 2 mm.

4.1. FLOOR ANALYSIS

A subset of floor points is extracted from each registered point cloud using the same manually designed geometric extraction shape. In the height direction (z-axis), a comparison is made with reference data. In Table 2 the statistical indices as the mean distance and their standard deviation values of the floor analysis are given.

Table 2. Statistics of C2C comparison between BLK360, SLAM, FJD TRION™ S1 and iPhone 12 Pro with the reference dataset - FARO Focus 3D in the z-axis.

System	Mean Distance (mm)	STD (mm)
Leica BLK360	7.8	4.9
GeoSLAM ZEB-REVO	11.3	8.3
iPhone 12 Pro	4.7	3.8
FJD TRION™ S1	25	10

According to the results, the point cloud generated by BLK360 is significantly denser (approx. three times) in comparison with SLAM results (see; Figure 4). Also, in terms of accuracy, the BLK Laser Scanner is superior compared to the GeoSLAM and FJD TRION™ S1 point cloud.

During our floor examination, we achieved a noteworthy result. By employing the C2C distance algorithm to a limited area of the floor's z-axis, we determined that the point cloud generated by the iPhone 12 Pro was more accurate and closer to the ground truth data than those extracted by the other devices we tested. This outcome was quite interesting. In Figure 4 we demonstrate four (4) scalar field values of C2C absolute distances (z) diagrams and their histograms for each method. An interesting result is the subplot in Figure 4-F which demonstrates an impressive number of points in a relatively close to the ground truth distance.

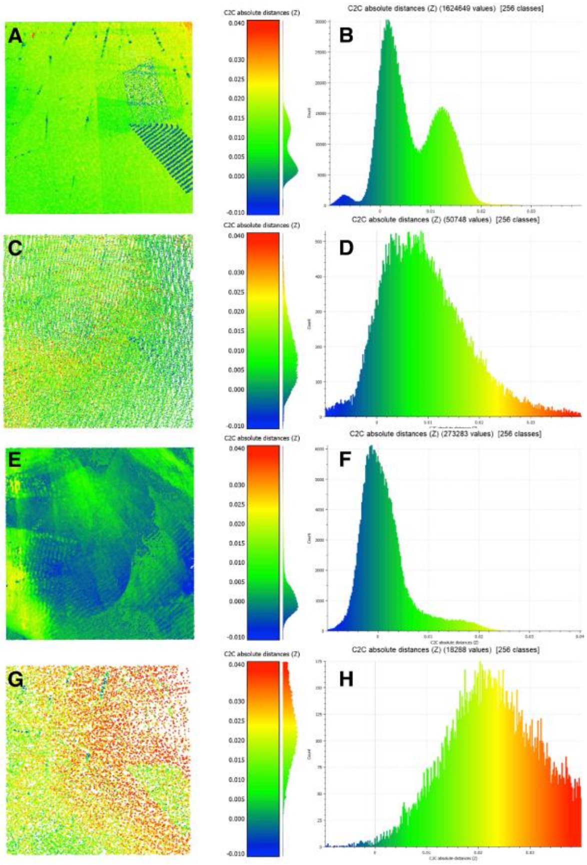

Figure 4. Floor analysis comparison (3 x 3 m) between a-b) BLK360 c-d) GeoSLAM e-f) iPhone point clouds g-h) FJD TRION™ S1 and their statistics (Drawings created in CloudCompare by the author).

4.2. SECTION ANALYSIS

Following the aforementioned procedure, we also conducted cloud-to-cloud distance measurements for two vertical sections of the monument. This additional analysis is aimed at providing a more comprehensive understanding of the variations in accuracy among the different systems used for capturing the object of our study. Similar to our previous analysis, we compared the output data from each system with the ground-truth dataset to evaluate the accuracy of each system.

Based on the results of our analysis, we can assess the strengths and limitations of each system and provide recommendations for selecting the most suitable systems for specific applications. These subsections present the findings of our cloud-to-cloud distance measurements for the two vertical sections of the monument with scalar field values that represent the C2C absolute distances. In Figure 5, the four (4) individual methods are illustrated, in the section analysis. As demonstrated in histograms of Figure 5, A and B cases are appearing more accurate due to the fact that most of the points are closer to the ground-truth, while C and D show larger local deviations, with many points falling in the 2–4 cm range.

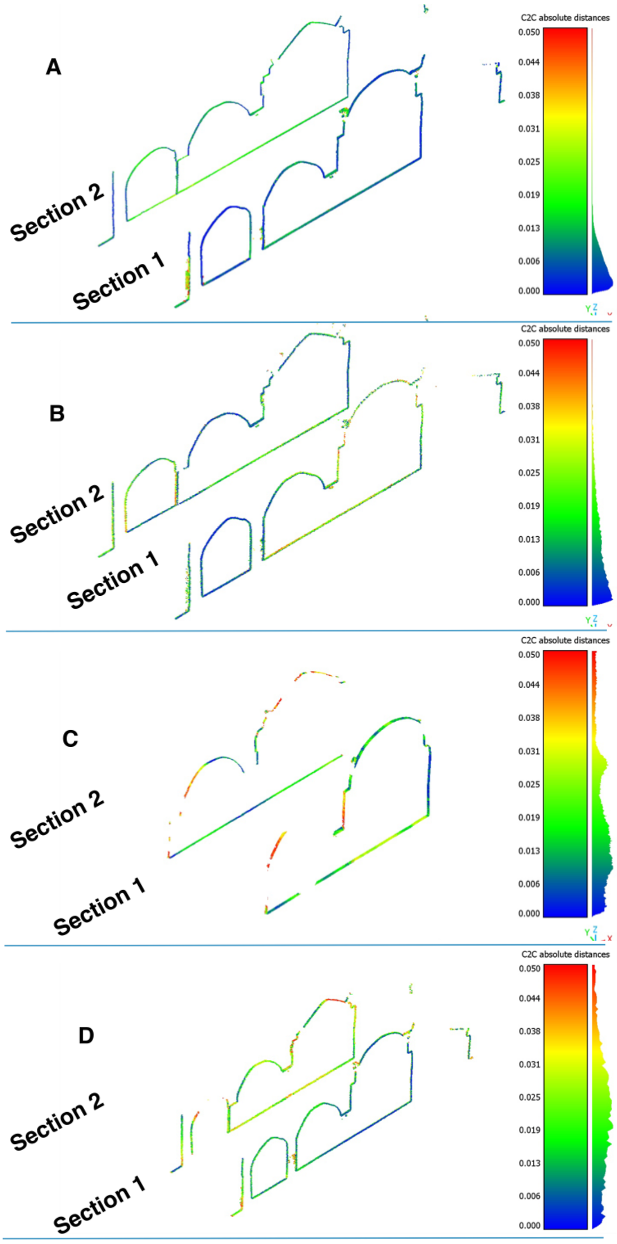

Figure 5. Section comparison between a) BLK360, b) GeoSLAM and c) iPhone 12 Pro d) FJD TRION™ S1 point clouds for sections 1-2 (Drawings created in CloudCompare by the author).

Table 3. Statistical comparison between a) BLK360, b) GeoSLAM c) iPhone 12 Pro and d) FJD TRION™ S1 for sections 1-2.

	System	Mean D. (mm)	STD (mm)
Section 1	Leica BLK360	8	11
	GeoSLAM ZEB-REVO	12	14
	iPhone 12 Pro	22	12
	FJD TRION™ S1	16	19
Section 2	Leica BLK360	10	8
	GeoSLAM ZEB-REVO	13	30
	iPhone 12 Pro	19	17
	FJD TRION™ S1	22	12

In Figure 6, we present the statistical comparison of section analysis between the four different measuring systems for sections 1-2. Regarding to mean distance differences and standard deviation, we realize that Leica BLK360 provides the most compatible results with the ground truth, with differences 8 ±11 mm and 10 ±8 mm for sections1-2 respectively. Should note that GeoSLAM ZEB-REVO gives the highest standard deviation in section 2, with value 13 ± 30 mm, that indicates the differences are more spread out.

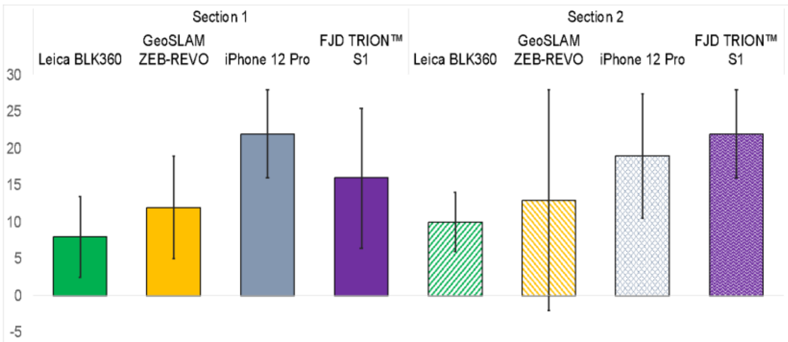

Figure 6. Statistical comparison between BLK360, GeoSLAM, iPhone 12 Pro and FJD TRION™ S1 for sections 1-2 (Diagram in Microsoft Excel by the author).

4.3. MULTISCALE MODEL TO MODEL CLOUD COMPARISON

Subsequently, we employed the M3C2 (Multiscale Model to Model Cloud Comparison) algorithm to compare the output data from the different systems used for capturing the environment. The M3C2 algorithm is a widely used and well-established method for point cloud comparison, which provides an accurate and robust analysis of differences between two or more-point cloud datasets [20].

The M3C2 algorithm is particularly useful for comparing point cloud data from different systems, as it provides a quantitative evaluation of differences between datasets, rather than relying solely on visual inspection. This allows for more objective and reliable assessments of the performance of different systems and enables a more robust comparison of their accuracy and efficacy. The use of the M3C2 algorithm provides a reliable and accurate method for comparing point cloud data from different systems [21]. Its ability to compare datasets at different scales, as well as its robustness to noise and errors, makes it a valuable tool for point cloud analysis in various applications. We used the M3C2 method in two parts of the monument. As a first step of our analysis, we focused on the external facet in the southern part of the monument, as illustrated in Figure 7. We selected this part of the monument due to the complex geometrical characteristics of its surface. We should note that in subplot B of Figure 7, the points marked in blue and red, respectively, show the points that are further away from the ground-truth. This is thought to be the effect of the laser beam's incidence angle.

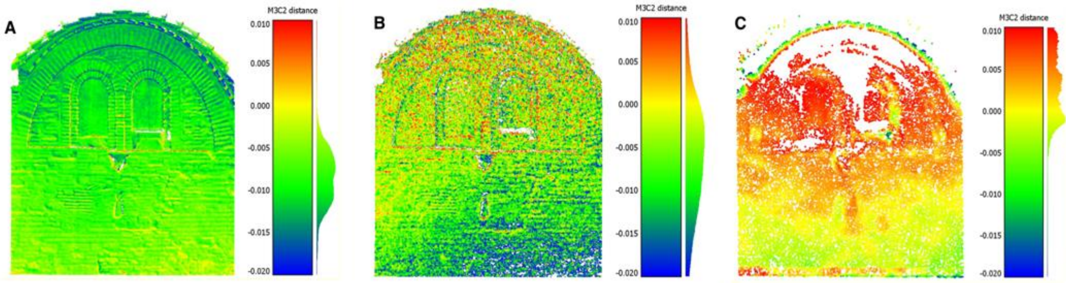

Figure 7. Comparison between a) BLK360 and b) GeoSLAM c) FJD TRION™ S1 using M3C2 algorithm (Drawings created in CloudCompare by the author).

Next, we performed the same procedure for a thick section of the internal part of the monument. In this step we are able to compare data with the ground truth using the M3C2 algorithm for all available systems [22]. In Figure 8 the most notable differences are detected in the point cloud from the iPhone 12 Pro. It is important to underline that the points with the red colour in the north-east part of the internal walls are the last part of the monument that was scanned with the iPhone iOS application. This is an expected outcome due to the fact that, in general, the longer the trajectory, the greater the potential of accumulated errors, drift, and uncertainty in the estimated positions and maps. This is because SLAM systems typically rely on integrating measurements from multiple sensors over time to estimate the device position and orientation relative to the environment, and to build a map of the environment. As the device moves over a longer trajectory, errors in the sensor measurements, inaccuracies in the device motion model, and uncertainties in the environment can accumulate, leading to a degradation in the accuracy of the estimated positions and maps.

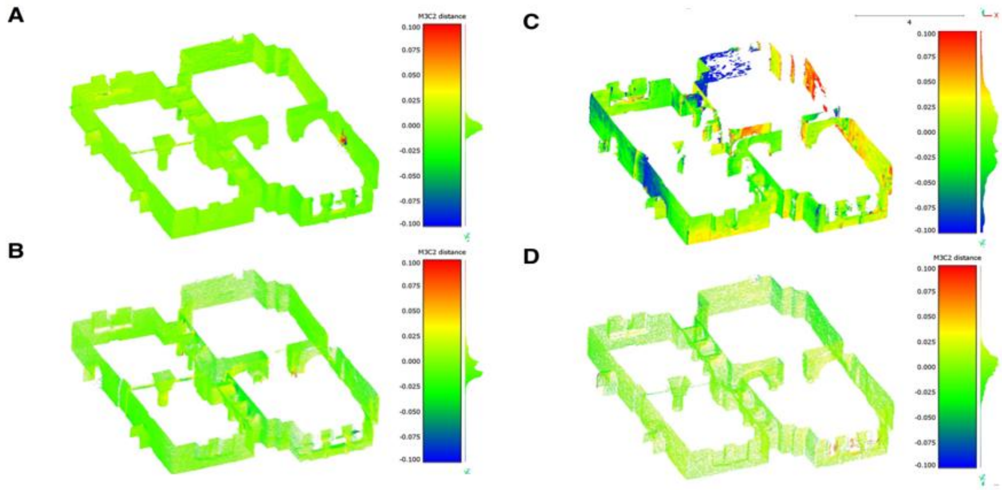

Figure 8. M3C2 distances of a thick section of the internal part of the monument between a) BLK360 and b) GeoSLAM and c) iPhone 12 Pro d) FJD TRION™ S 1 (Drawings created in CloudCompare by the author).

5. CONCLUSIONS

Our experiments show that when we used the C2C distance algorithm in the full models the expensive and professional surveying instruments were superior by far to Apple's 3D point cloud result. When we studied the accuracy of the sections, the result from Apple's LiDAR is not extremely disappointing compared to the TLS and SLAM professional equipment but still there is a significant difference. The BLK360, GeoSLAM ZEB Revo and FJD TRION™ S1 have been specifically designed for the purpose of 3D point cloud data capturing, whereas the iPhone 12 Pro is a multipurpose device that has a LiDAR sensor as an additional feature. Therefore, while the iPhone 12 Pro can be used for point cloud 3D mapping, the rest provide superior options due to their specialised features and purpose-built design. The results were similar also when we used the Multiscale Model to Model Cloud Comparison for a part of the internal part of the monument.

However, we obtained an intriguing result in the "Floor Analysis". We applied the C2C distance algorithm along the z-axis for a small part of the floor and showed that the point cloud extracted from iPhone 12 was closer to the ground-truth than the others. We assume that this is related to the position of the iPhone in relation to the floor. The LiDAR beam direction of the iPhone was collinear to the direction of the coordinates in study (height-Z) at a small distance (more or less than 1m) while the iPhone's imaging sensor was parallel to the floor. On the other hand, the position of the scanner and the slam systems were measuring points on the floor from longer distances and the ranging laser beams were emitted in varying angles relative to the floor normal. There are promising expectations for the upcoming years from two standpoints: the development of devices and software. In terms of device development, Apple's decision to include a LiDAR sensor in their products is significant and showcases the growing interest in this technology for low-cost devices intended for mass consumption, in comparison to more expensive TLS devices. As for software development, the potential market for utilizing mobile devices in 3D metric surveying is already emerging, with software companies releasing surveying software that is specifically geared towards leveraging the Apple LiDAR sensor.

The optimal methodologies for documenting procedures spanning from data acquisition to the final product, utilizing TLS and SLAM equipment, primarily involve the former. It has been evidenced that terrestrial laser scanning is efficaciously applicable for documenting cultural heritage characterized by intricate geometries and irregular shapes. Nevertheless, the inquiry has substantiated that SLAM technology exhibits considerable promise in delivering viable and pertinent outcomes within challenging field environments, facilitating expeditious and timely surveys.

LITERATURE

[1] F. Revithiadou and K. Raptis, Restoration - Consolidation of the Byzantine Bath in Thessaloniki. Thessaloniki: Ziti Publ., 2014.

[2] G. Luetzenburg, A. Kroon, and A. A. Bjørk, "Evaluation of the Apple iPhone 12 Pro LiDAR for an Application in Geosciences," *Scientific Reports*, vol. 11, no. 1, p. 22221, Nov. 2021, doi: https://doi.org/10.1038/s41598-021-01763-9.

[3] G. Vacca, "3D Survey with Apple LiDAR Sensor—Test and Assessment for Architectural and Cultural Heritage," *Heritage*, vol. 6, no. 2, pp. 1476–1501, Feb. 2023, doi: https://doi.org/10.3390/heritage6020080.

[4] T. P. Kersten and M. Lindstaedt, "Geometric accuracy investigations of terrestrial laser scanner systems in the laboratory and in the field," *Applied Geomatics*, May 2022, doi: https://doi.org/10.1007/s12518-022-00442-2.

[5] S. Soudarissanane, R. Lindenbergh, M. Menenti, and P. Teunissen, "Scanning geometry: Influencing factor on the quality of terrestrial laser scanning points," *ISPRS Journal of Photogrammetry and Remote Sensing*, vol. 66, no. 4, pp. 389–399, 2011.

[6] A. Kharroubi, F. Poux, Z. Ballouch, R. Hajji, and R. Billen, "Three Dimensional Change Detection Using Point Clouds: A Review," *Geomatics*, vol. 2, no. 4, pp. 457–485, Dec. 2022, doi: https://doi.org/10.3390/geomatics2040025.

[7] M. Ingman, J.-P. Virtanen, M. T. Vaaja, and H. Hyyppä, "A Comparison of Low-Cost Sensor Systems in Automatic Cloud-Based Indoor 3D Modeling," *Remote Sensing*, vol. 12, no. 16, p. 2624, Aug. 2020, doi: https://doi.org/10.3390/rs12162624.

[8] Leica Geosystems. "BLK360 3D Laser Scanner User Manual." Leica Geosystems. Accessed: Jan. 18, 2025. [Online]. Available: https://leica-geosystems.com/products/laser-scanners

[9] FARO. "Focus 3D Laser Scanner User Manual." FARO. Accessed: Jan. 18, 2025. [Online]. Available: https://downloads.faro.com/index.php/s/CY5BS9Jd2JEf8YY

[10] FJDynamics. "FJDynamics User Manual." FJDynamics. Accessed: Jan. 18, 2025. [Online]. Available: https://www.fjdynamics.com

[11] C. Gollob, T. Ritter, and A. Nothdurft, "Comparison of 3D Point Clouds Obtained by Terrestrial Laser Scanning and Personal Laser Scanning on Forest Inventory Sample Plots," *Data*, vol. 5, no. 4, p. 103, Oct. 2020, doi: https://doi.org/10.3390/data5040103.

[12] G. Lin, A. Giordano, K. Sang, L. Stendardo, and X. Yang, "Application of Terrestrial Laser Scanning in 3D Modelling of Traditional Village: A Case Study of Fenghuang Village in China," 2021.

[13] S. Bitharis, C. Pikridas, B. Tsioukas, I.-A. Karolos, and K. Bellos, "The Contribution of Three-Dimensional Recording of Industrial Infrastructure with Emphasis on Creating a Three-Dimensional Photorealistic Model," *Chorografies*, no. 9, 2022, doi: https://doi.org/10.26234/HEAL.IHU.GJFQ-R082.

[14] R. C. Smith and P. Cheeseman, "On the Representation and Estimation of Spatial Uncertainty," *The International Journal of Robotics Research*, vol. 5, no. 4, pp. 56–68, Dec. 1986, doi: https://doi.org/10.1177/027836498600500404.

[15] Leica Geosystems. "Leica Cyclone FIELD 360." Leica Geosystems. Accessed: Jan. 18, 2025. [Online]. Available: https://leica-geosystems.com/products/laser-scanners/scanners/leica-rtc360

[16] P. J. Besl and N. D. McKay, "Method for registration of 3-D shapes," in *Proc. SPIE 1611, Sensor Fusion IV: Control Paradigms and Data Structures*, Apr. 1992, doi: https://doi.org/10.1117/12.57955.

[17] M. Shanoer and F. M. Abed, "Evaluate 3D laser point clouds registration for cultural heritage documentation," *The Egyptian Journal of Remote Sensing and Space Science*, vol. 21, no. 3, pp. 295–304, Dec. 2018, doi: https://doi.org/10.1016/j.ejrs.2017.11.007.

[18] L. Teppati Losè, A. Spreafico, F. Chiabrando, and F. Giulio Tonolo, "Apple LiDAR Sensor for 3D Surveying: Tests and Results in the Cultural Heritage Domain," *Remote Sensing*, vol. 14, no. 17, p. 4157, 2022, doi: https://doi.org/10.3390/rs14174157.

[19] A. Photo. "3D Scanner App." App Store. Accessed: Jan. 20, 2026. [Online]. Available: https://apps.apple.com/us/app/3d-scanner-app/id1419913995

[20] D. Lague, N. Brodu, and J. Leroux, "Accurate 3D comparison of complex topography with terrestrial laser scanner: Application to the Rangitikei canyon (N-Z)," *ISPRS Journal of Photogrammetry and Remote Sensing*, vol. 82, pp. 10–26, Aug. 2013, doi: https://doi.org/10.1016/j.isprsjprs.2013.04.009.

[21] L. Winiwarter and B. Höfle, "M3C2-EP: Pushing the limits of 3D topographic point cloud change detection by error propagation," *ISPRS Journal of Photogrammetry and Remote Sensing*, vol. 178, pp. 240–258, Aug. 2021, doi: https://doi.org/10.1016/j.isprsjprs.2021.06.011.

[22] P.-M. DiFrancesco, D. Bonneau, and D. J. Hutchinson, "The Implications of M3C2 Projection Diameter on 3D Semi-Automated Rockfall Extraction from Sequential Terrestrial Laser Scanning Point Clouds," *Remote Sensing*, vol. 12, no. 11, p. 1885, Jun. 2020, doi: https://doi.org/10.3390/rs12111885.